Conference Paper, Published Version

Onda, Shinichiro; Shirai, H.; Hosoda, Takashi; Arimitsu, T.; Ooe, K.

Numerical simulation of river channel processes with bank erosion in steep curved channel

River Flow 2010 - Dittrich, Koll, Aberle & Geisenhainer (eds) - © 2010 Bundesanstalt für Wasserbau ISBN 978-3-939230-00-7

Numerical simulation of river channel processes with bank erosion in steep curved channel

S. Onda, H. Shirai & T. Hosoda
Department of Urban Management, Kyoto University, Kyoto, Japan

T. Arimitsu & K. Ooe
The Kansai Electric Power Co., Inc., Amagasaki, Hyogo, Japan

ABSTRACT: Accurate estimation of sediment inflow into reservoir is of great importance for an efficient dam management. The sediment supply is mainly caused by excessive bank erosion in mountainous rivers during floods. In this study, a numerical model which combines a depth averaged flow model in generalized curvilinear coordinate system and equilibrium and non-equilibrium sediment transport models is applied to river channel processes with bank erosion in steep curved channel. The bank collapse process is also considered by a simplified failure model. The applicability of the numerical model is examined through the comparison with previous experimental results.

Keywords: Bank erosion, Equilibrium and non-equilibrium sediment transport models, Numerical simulation, Generalized curvilinear coordinate system

1 INTRODUCTION

Accurate prediction of sediment inflow into reservoir is of great importance for an efficient dam management. The sediment supply is mainly caused by excessive bank erosion in mountainous river reaches during floods. In addition, a complex bed deformation can be observed in a curved channel due to secondary currents. Therefore, it is necessary to predict river channel processes with bank erosion in curved channel accurately for an effective management.

A number of theoretical and experimental studies concerning the bed deformation and bank line shifting in straight and meandering channels have been conducted (e.g. Kovacs and Parker 1994, Seminara 2006, Shimizu et al. 1996). Moreover, some numerical models considering bed deformation with bank erosion have been proposed (e.g. Nagata et al. 1996, 2000, Sekine 1996, Shimizu et al. 1996, Shimizu 2004). However, these models are mainly applied to alluvial channels with mild slope and their applicability to the cases with steep slope is not examined enough.

On the other hand, in the previous studies concerning the bed deformation for upper regime flow, Meguro et al. (2001) conducted the hydraulic experiments in the straight channel and reported that multi-scale sand waves from micro- to large scale are formed. Arimitsu et al. (2009) carried out the hydraulic experiments in steep curved channel with fixed and movable beds. In the case of fixed bed, characteristics of water surface oscillations due to shock waves were investigated. It was also shown that multi-scale sand waves such as antidunes and bars can be observed in the movie, although the general characteristics of bed deformation in equilibrium stage are similar to the results for lower regime flow in the previous studies. In simulation of flow and bed deformation for upper regime flow, a one-dimensional model is commonly used to predict the large scale bed deformation in the longitudinal direction. Therefore, applicability of a depth averaged two-dimensional flow model is not examined. Hence, to simulate flow and bed deformation in steep curved channel, it is necessary to reproduce development of secondary currents, formation of point bar and non-equilibrium state of sediment near river bank.

In this study, a numerical model to simulate river channel processes with bank erosion in steep curved channel is examined, using a depth averaged flow model in generalized curvilinear coordinate system and both equilibrium and non-equilibrium sediment transport models. In the non-equilibrium sediment transport model, sediment movements of bed load are characterized with pick-up rate and step length, while the em-

pirical formula is used in the equilibrium sediment transport model. The bank collapse process is also considered by a simplified failure model. The model is verified through the comparison between experimental and numerical results.

2 NUMERICAL MODEL

2.1 *Basic equations of flow*

A depth averaged flow model in generalized curvilinear coordinate system is used to calculate flow fields.

[Continuity equation]

$$\frac{\partial}{\partial t}\left(\frac{h}{J}\right)+\frac{\partial}{\partial \xi}\left(\frac{Uh}{J}\right)+\frac{\partial}{\partial \eta}\left(\frac{Vh}{J}\right)=0 \tag{1}$$

[Momentum equation]

$$\begin{aligned}
&\frac{\partial}{\partial t}\left(\frac{Q^{\xi}}{J}\right)+\frac{\partial}{\partial \xi}\left(\frac{UQ^{\xi}}{J}\right)+\frac{\partial}{\partial \eta}\left(\frac{VQ^{\xi}}{J}\right)\\
&-\frac{M}{J}\left(U\frac{\partial \xi_x}{\partial \xi}+V\frac{\partial \xi_x}{\partial \eta}\right)-\frac{N}{J}\left(U\frac{\partial \xi_y}{\partial \xi}+V\frac{\partial \xi_y}{\partial \eta}\right)\\
&=-gh\left(\frac{\xi_x^2+\xi_y^2}{J}\frac{\partial z_s}{\partial \xi}+\frac{\xi_x\eta_x+\xi_y\eta_y}{J}\frac{\partial z_s}{\partial \eta}\right)-\frac{\tau_b^{\xi}}{\rho J}\\
&+\frac{\xi_x^2}{J}\frac{\partial}{\partial \xi}\left(-\overline{u'^2}h\right)+\frac{\xi_x\eta_x}{J}\frac{\partial}{\partial \eta}\left(-\overline{u'^2}h\right)\\
&+\frac{\xi_y^2}{J}\frac{\partial}{\partial \xi}\left(-\overline{v'^2}h\right)+\frac{\xi_y\eta_y}{J}\frac{\partial}{\partial \eta}\left(-\overline{v'^2}h\right)\\
&+\frac{2\xi_x\xi_y}{J}\frac{\partial}{\partial \xi}\left(-\overline{u'v'}h\right)+\frac{\xi_x\eta_y+\xi_y\eta_x}{J}\frac{\partial}{\partial \eta}\left(-\overline{u'v'}h\right)
\end{aligned} \tag{2a}$$

$$\begin{aligned}
&\frac{\partial}{\partial t}\left(\frac{Q^{\eta}}{J}\right)+\frac{\partial}{\partial \xi}\left(\frac{UQ^{\eta}}{J}\right)+\frac{\partial}{\partial \eta}\left(\frac{VQ^{\eta}}{J}\right)\\
&-\frac{M}{J}\left(U\frac{\partial \eta_x}{\partial \xi}+V\frac{\partial \eta_x}{\partial \eta}\right)-\frac{N}{J}\left(U\frac{\partial \eta_y}{\partial \xi}+V\frac{\partial \eta_y}{\partial \eta}\right)\\
&=-gh\left(\frac{\xi_x\eta_x+\xi_y\eta_y}{J}\frac{\partial z_s}{\partial \xi}+\frac{\eta_x^2+\eta_y^2}{J}\frac{\partial z_s}{\partial \eta}\right)-\frac{\tau_b^{\eta}}{\rho J}\\
&+\frac{\xi_x\eta_x}{J}\frac{\partial}{\partial \xi}\left(-\overline{u'^2}h\right)+\frac{\eta_x^2}{J}\frac{\partial}{\partial \eta}\left(-\overline{u'^2}h\right)\\
&+\frac{\xi_y\eta_y}{J}\frac{\partial}{\partial \xi}\left(-\overline{v'^2}h\right)+\frac{\eta_y^2}{J}\frac{\partial}{\partial \eta}\left(-\overline{v'^2}h\right)\\
&+\frac{\xi_x\eta_y+\xi_y\eta_x}{J}\frac{\partial}{\partial \xi}\left(-\overline{u'v'}h\right)+\frac{2\eta_x\eta_y}{J}\frac{\partial}{\partial \eta}\left(-\overline{u'v'}h\right)
\end{aligned} \tag{2b}$$

where t = time; ξ, η = generalized curvilinear coordinates; J = Jacobian of coordinate transformation (= $1/(x_\xi y_\eta - x_\eta y_\xi)$); ξ_x, ξ_y, η_x, η_y = metrics of coordinate transformation; Q^{ξ}, Q^{η} = contravariant components of discharge flux vectors for unit width; M, N = Cartesian components of discharge flux vectors; U, V = contravariant components of velocity vectors; h = depth; z_s = water surface elevation from datum plane; g = gravitational acceleration; ρ = density of water; τ_b^{ξ}, τ_b^{η} = contravariant components of bottom shear stress vectors; $-\overline{u'^2}$,$-\overline{u'v'}$,$-\overline{v'^2}$ = Cartesian components of Reynolds stress tensors.

2.2 *Equilibrium sediment transport model*

To evaluate bed load fluxes in the streamwise and transversal directions, the following formula proposed by Ashida and Michiue (1972), Hasegawa (1984) are used.

$$q_{bs}=17\tau_{*e}^{\frac{3}{2}}\left(1-\frac{\tau_{*c}}{\tau_*}\right)\left(1-\frac{u_{*c}}{u_*}\right)\sqrt{(\sigma/\rho-1)gd^3} \tag{3a}$$

$$q_{bn}=q_{bs}\left(\frac{u_{n_b}}{u_{s_b}}-\sqrt{\frac{\tau_{*c}}{\mu_s\mu_k\tau_*}}\frac{\partial z_b}{\partial n}\right) \tag{3b}$$

$$u_{n_b}=-N_*\frac{h}{r}u_{s_b},\quad (N_*=8.5) \tag{3c}$$

where q_{bs}, q_{bn} = bed load flux vectors in the streamwise and transversal directions; τ_{*e}, τ_{*c}, τ_* = non-dimensional effective shear stress, critical shear stress and shear stress, respectively; u_*, u_{*c} = friction velocity and critical friction velocity; d = diameter of sand; σ = density of sand (σ/ρ=2.65); u_{s_b}, u_{n_b} = the velocity components in the streamwise and transversal direction near the bottom; μ_s and μ_k = static and kinetic friction coefficient of bed material, respectively (=1.0, 0.5).

The bed elevation is calculated using following continuity equation after transforming in the contravariant components of bed load flux vectors ($q_{b\xi}$, $q_{b\eta}$).

$$\frac{\partial}{\partial t}\left(\frac{z_b}{J}\right)+\frac{1}{1-\lambda}\left\{\frac{\partial}{\partial \xi}\left(\frac{q_{b\xi}}{J}\right)+\frac{\partial}{\partial \eta}\left(\frac{q_{b\eta}}{J}\right)\right\}=0 \tag{4}$$

where z_b = bed elevation; λ = porosity of sand (=0.4).

2.3 *Non-equilibrium sediment transport model*

A non-equilibrium sediment transport model (Nagata et al. 2000) consists of 4 steps; (1) evaluation of pick-up rate, (2) calculation of trajectory of sand, (3) calculation of deposition rate and (4) temporal change of bed level. The pick-up rate is evaluated in the following equation proposed by Nakagawa et al. (1986), which can be applicable to the channel with side slope.

Table 1. Hydraulic conditions

	Discharge Q (m^3/s)	Width B (m)	Water depth h (m)	Bed slope	Radius of curvature r (m)	Diameter of sand d (mm)
Case A	0.0085	0.5	0.024	1/80	2.0	1.86
Case B	0.0085	1.0	0.016	1/80	2.0	1.86

Table 2. Computational conditions

	Case	Sediment transport model	step length Λ (mm)	Angle of repose under water surface	Angle of repose at the edge of water
Run1-1	A	Equilibrium model		25°	65°
Run1-2	A	Non-equilibrium model	50d	15°	65°
Run1-3	A	Non-equilibrium model	100d	15°	65°
Run1-4	A	Non-equilibrium model	250d	15°	65°
Run2-1	B	Equilibrium model		25°	65°
Run2-2	B	Non-equilibrium model	100d	15°	65°

$$p_s\sqrt{\frac{d}{(\sigma/\rho-1)g}}=F_0G_*\tau_*\left(1-\frac{k_2\Omega\tau_{*c}}{\tau_*}\right)^m$$
$$G_*=\frac{\cos\psi+k_L\mu_s}{1+k_L\mu_s} \quad (5)$$
$$\Omega=\left(\frac{\mu_s\cos\theta_n-\sin\theta_n\sin\phi}{\cos\psi+k_L\mu_s}\right)\left(\frac{1+k_L\mu_s}{\mu_s}\right)$$

where p_s = pick-up rate; k_L = ratio of lift force to drag force (=0.85, Chepil 1958); ψ = angle between velocity vector near bed and sediment movement direction; θ_n = local bed slope angle; ϕ = angle between streamwise direction and sediment movement direction; and F_0, k_2, and m = constants (=0.03, 0.7, and 3, respectively). The detailed method to obtain the angles ψ and ϕ is described in the reference (Nagata et al. 2000) and the angle θ_n is calculated using the value of bed elevation between four neighboring cells.

Then, using bed load fluxes in the streamwise and transversal directions calculated in Equation (3), the direction of sediment movement and the distance from the pick-up point can be found, and the sediment deposition rate with distance increment of Δs = 0.01m is calculated. The deposition rate $p_{d\,(j,i)}$ on the locus after i-th point since being picked up at point j is obtained by the following equation.

$$p_{d(j,i)}=p_{s(j)}f_s\left(s_{(i)}\right)\Delta s\frac{A_{(j)}}{A_{(i)}} \quad (6a)$$

$$f_s(s)=\frac{1}{\Lambda}\exp\left(-\frac{s}{\Lambda}\right) \quad (6b)$$

$$s_{(i)}=i\cdot\Delta s \quad (6c)$$

where $A_{(j)}$, $A_{(i)}$ = numerical mesh areas at the positions of pick-up and deposition rates; Δs = length increment for calculation of the locus; and $f_s(s)$ = probability density function of step length; Λ = average step length, which is proportional to sand diameter (=αd). The value of step length Λ is generally reported to vary from 50d to 250d, and the averaged value is 100d (Nakagawa and Tsujimoto 1980). Therefore, various values of step length are applied to examine the effects of step length. It should be noted that since the position of deposition rate is not coincident with the pick-up rate, the deposition rate is distributed to the position where pick-up rate is defined.

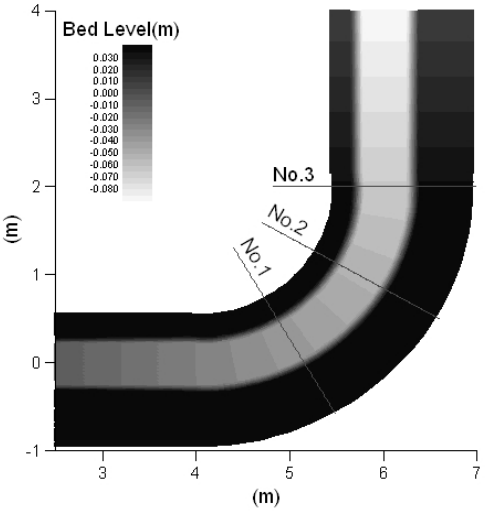

Figure 1. Initial bed level in Case A

Using the pick-up and deposition rate calculated in Equations (5) and (6), the temporal change of bed elevation is obtained by the following equation (Nakagawa and Tsujimoto 1980).

$$\frac{\partial z_b}{\partial t}=A_1d\left(p_d-p_s\right) \quad (7)$$

where A_1 = one-dimensional geometrical coefficient of sand (=1.0).

2.4 *Bank failure model*

When bed near the edge of the channel bank is scoured, bank collapses intermittently due to instability of side bank. A simplified bank failure

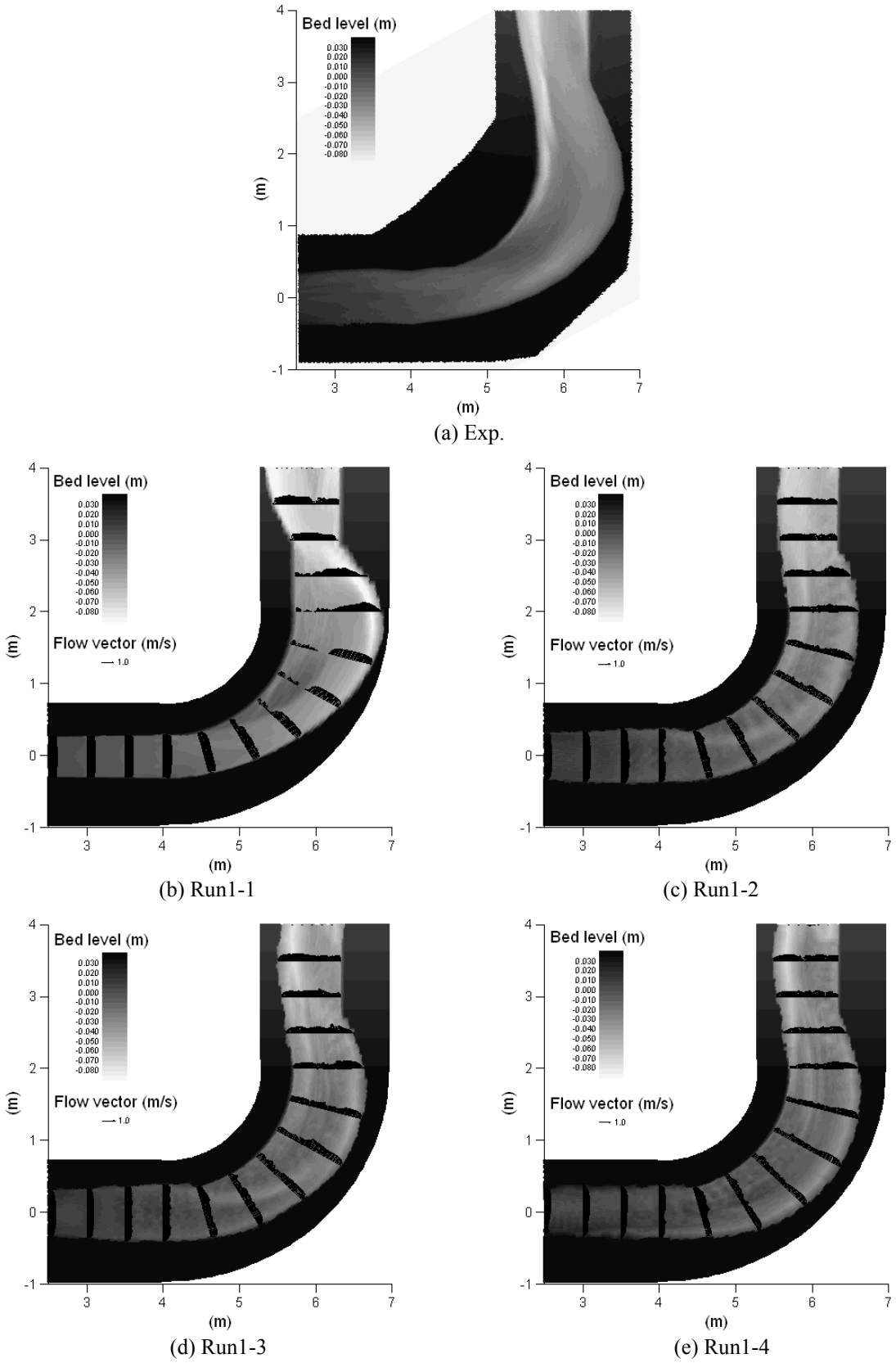

Figure 2. Bed level contours and velocity vectors in Case A

model is used in the numerical simulation, although various models are proposed (e.g. Hasegawa 1984, Nagata et al. 2000, Shimizu 2004). The calculation of bank erosion is carried out when local bed slope between eight neighboring cells becomes steeper than the angle of repose of the bed material. It is assumed that volume of bank collapse becomes equal to the volume of deposition in the neighboring cells. Here, different values of the angle are used depending on condition, that both adjacent cells are under water surface or that the cell of fellow is under water surface (at the edge of the water). By using this simplified failure model, the characteristics of steep form at the river bank observed in the experiments after bank failure can be simulated. In this

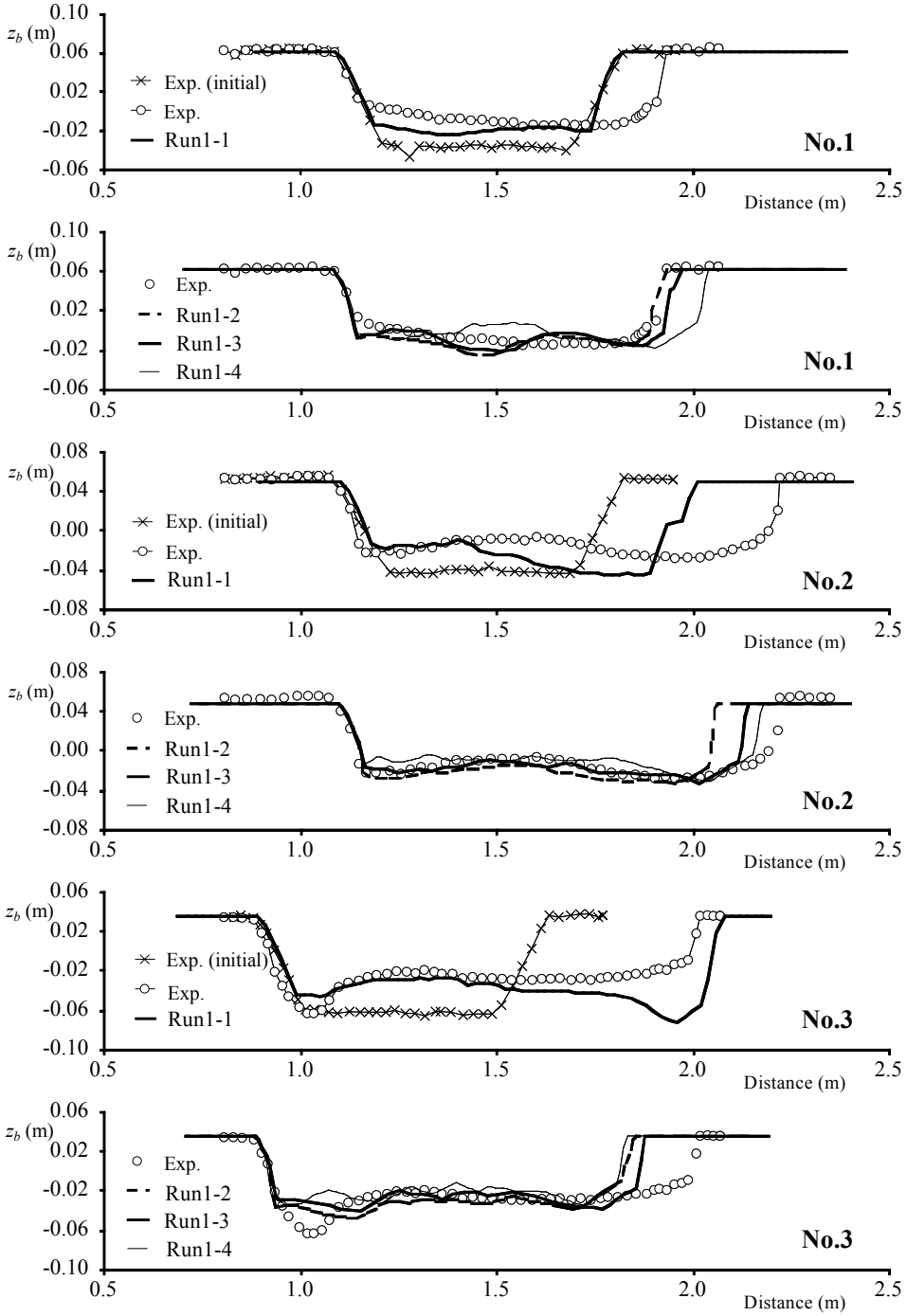

Figure 3. Comparison of bed variations in the transversal direction in Case A

model, the shape of grids may affect the results since the direction of bank failure is calculated from the eight neighboring cells. On the other hand, Sekine (2004) has proposed a bank failure model in which the direction of bank collapse is calculated explicitly. Further investigation for the treatment of bank collapse is needed.

3 COMPUTATIONAL CONDITIONS

The numerical model is applied to the previous experiments conducted by Arimitsu et al. (2009), and the applicability of both equilibrium and non-equilibrium sediment transport models is examined. The bed slope of channel in the experiments is 1/80 and radius of curvature r is 2.0m. The cross section of channel is trapezoidal with side slope of 40^o. The hydraulic conditions are summarized in Table 1. The two cases are simulated with small width (B = 0.5m, r/B = 4.0) and large width (B = 1.0m, r/B = 2.0). The computational conditions are shown in Table 2 and the initial bed level with small width is presented in Figure 1.

The governing equations are discretized in space using the finite volume method in which Adams-Bashforth method is applied for time integration and QUICK-scheme (Leonard 1979) is implemented for convection terms. The computational mesh size in the streamwise direction is 0.05m in straight and 1.5^o in curved channel

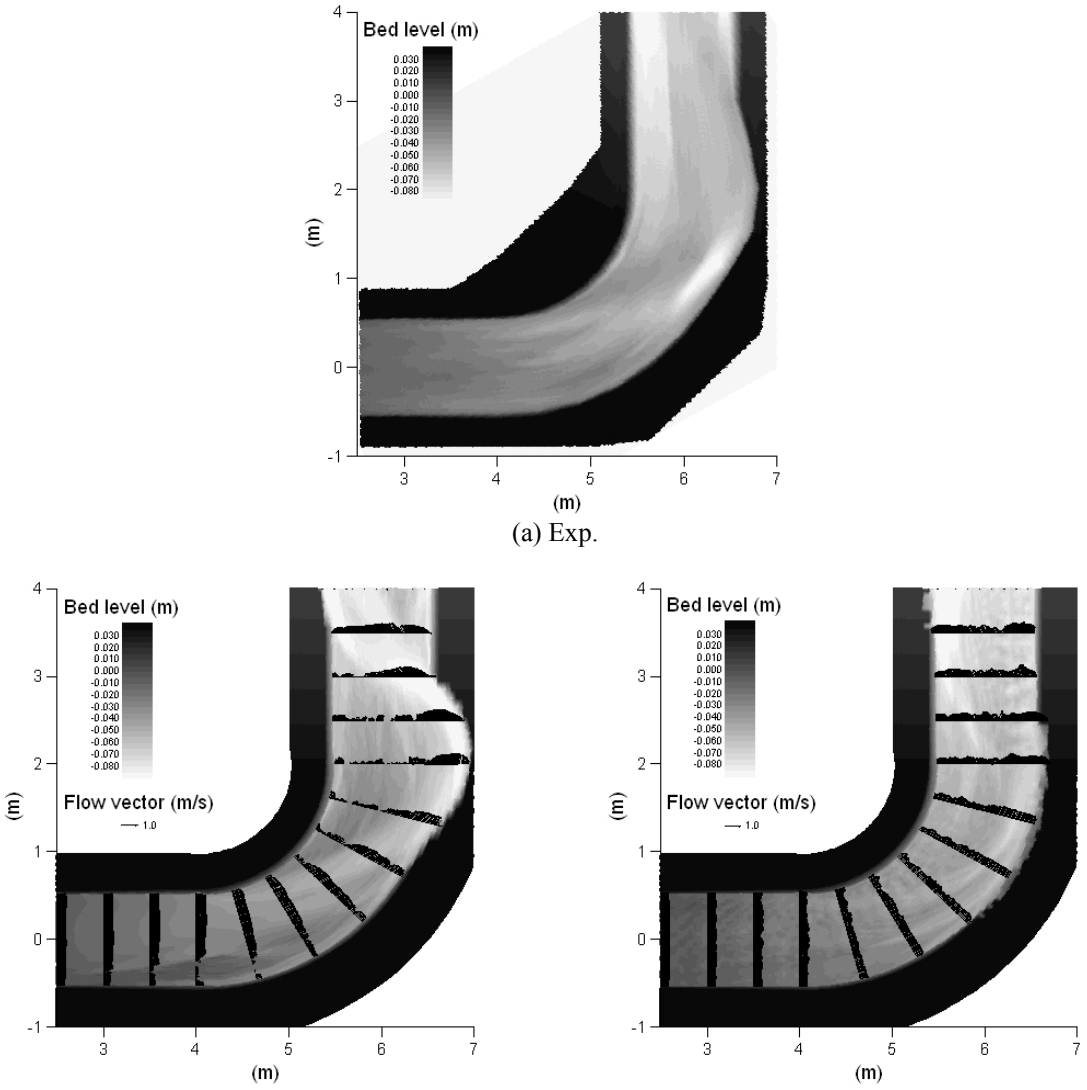

Figure 4. Bed level contours and velocity vectors in Case B

respectively, and the size in the transversal direction is 0.01m.

4 RESULTS AND DISCUSSION

Firstly, it is necessary to adjust two parameters for the angles of repose of bed materials under the water surface or at the edge of the water. The sensitivity analysis for the angle of repose of the bed material was carried out using the equilibrium sediment transport model (Figures are not shown). While the angle of repose of the bed material is generally reported to be 30^o, it is thought that the angle with bank erosion depends on the hydraulic condition and characteristics of bed materials, as pointed by Goto et al. (2001). Therefore, numerical experiments are conducted using the same value for the angle of repose at the edge of the water and the different values for the one under the water surface. The angle of repose near river bank is set to be 65^o since banks tend to be almost vertical in the experiments. In the case of large value for the angle of repose under the water surface (e.g. 30^o), the sediments due to the bank collapse are not supplied from the river bank, rather the bed in the outer bank is scoured. Consequently, bed degradation in outer bank can be observed and river bank is not shifted outward. On the other hand, in the case of small value for the angle, the sediments are supplied from the river bank after the bed in the outer bank is scoured. As a result, extensive bank erosion can be observed. In this study, the different values for angle of repose shown in Table 2 are used between the equilibrium and the non-equilibrium sediment transport models to reproduce the position of river bank at the 90^o section in the curved channel, which are smaller than the standard value (30^o). To determine the suitable parameter, further investigation is required.

Figure 2 represents comparison of bed level contours in the case of small width and Figure 3 is comparison of bed level in the transversal direction at 3 different sections (30^o, 60^o and 90^o) in the curved channel as shown in Figure 1. In the

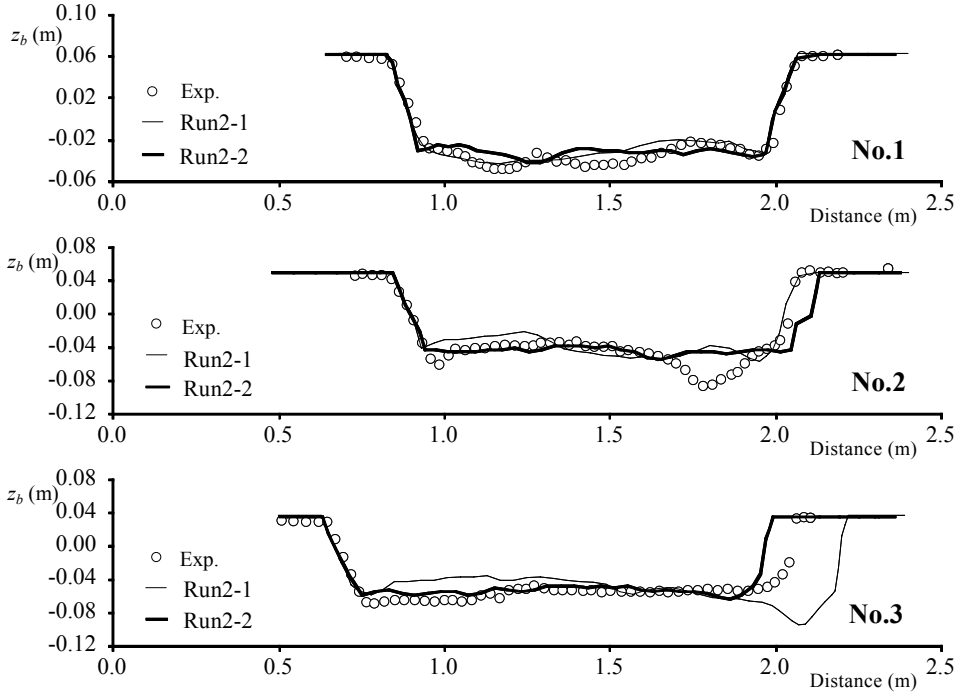

Figure 5. Comparison of bed variation in the transversal direction in Case B

experimental results, the point bar is formed at the inner bank of the curved channel and the river bed at outer bank is scoured. Moreover, the bank erosion occurs at outer bank in curved channel and sediment deposition due to secondary currents at the same section can be observed. The position of river bank at No.3 section in the curved channel can be reproduced by using the adjusted angle of repose in Run1-1 (equilibrium sediment transport model), while agreement between experimental and numerical results at the outer bank in the upstream side is not so satisfactory. The bed scouring at the inner bank in the downstream side of curved channel also cannot be simulated well.

Next, the numerical results in the non-equilibrium sediment transport model (Run1-2, 1-3 and 1-4) are compared with experiments. In the case of Run1-2 in which the averaged step length is short, the picked up sediments tend to deposit at closer point, and the characteristics of bed scouring in the outer bank and bank line shift can not be simulated well. In Run1-4, the peak of bank erosion point is occurred in the upstream side of curved channel compared with the experiments, and the bed variations in the downstream side are not reproduced. On the other hand, the bed elevations at No.1 and 2 sections in Run1-3 can be reproduced satisfactorily by using the appropriate averaged step length, while the position of river bank at 90^o can not be simulated rather. It is also observed that the bed scouring at the inner bank in the downstream of curved channel can be also simulated well in Run1-3. These results are thought to be related to the non-equilibrium condition of sediments near river bank as pointed out by Nagata et al. (2000). Near the river bank, side slope in transversal direction is steep and the sediments move from river bank to center of channel. Before bank erosion occurs intermittently, sediments are not supplied from bank. Consequently, non-equilibrium condition of sediments prevails. In the equilibrium sediment transport model, the bed load fluxes are calculated by using the local hydraulic variables in Equations (3). The condition of no flux in the transversal direction is not considered before the bank erosion occurs. Therefore, the bed load flux is overestimated, although the actual flux is small. It can be concluded that modeling of sediment movements is considered more accurately in the non-equilibrium model. The development processes of antidunes which are observed in the movie of experiments were not reproduced in this numerical simulation. It is due to the fact that a simple depth averaged flow model is applied to calculate the flow fields. Therefore, the improvement of flow model to a Boussinesq equation considering the effects of vertical acceleration is required.

Figures 4 and 5 show comparison of the bed contours and the bed elevation in the transversal direction in the case of large width. In this case, since the bed variation is so small and the river bank is not shifted much, both types of sediment transport models can simulate the bed deformation. Moreover, the characteristics that the peak position of bank erosion occurs in the downstream side compared with the small width case is reproduced well.

5 CONCLUSIONS

In this study, river channel processes in a curved channel with steep slope are simulated, using a depth averaged flow model in generalized curvilinear coordinate system. Equilibrium and non-equilibrium sediment transport models are employed and their applicability is examined. It is found that both types of sediment transport models can reproduce the experimental results by using the value of appropriate angle of repose. It should be noted that better agreement can be observed in the results of the non-equilibrium sediment transport model, especially in the case that the bank erosion progresses. In the future, to examine the effect of model scale in the numerical models between the equilibrium and non-equilibrium sediment transport model, the numerical models should be applied to the real scale of rivers. In addition, to indicate superiority in the non-equilibrium sediment transport model, further investigation is required by comparing the trajectory of sediments with experiments (e.g. from where to where and its rate of pick-up and deposition).

REFERENCES

Arimitsu, T., Kageyama, M., Deguchi, T., Fujita, I. and Moriyama, Y. 2008. Experimental study on flow and bank erosion in steep and curved trapezoidal channels. Proc. of 8th ICHE, (CD-ROM).

Arimitsu, T., Ooe, K., Onda, S., Hosoda, T. and Shirai, H. 2009. Experimental and numerical investigation of river channel processes with bank erosion in steep curved channel. River, Coastal and Estuarine Morphdynamics: RCEM2009, 2, 983-988.

Ashida, M. and Michiue, M. 1972. Study on hydraulic resistance and bed-load transport rate in alluvial streams. Proc. of JSCE, 206, 59-69 (in Japanese).

Chepil, W.S. 1958. The use of evenly spaced hemispheres to evaluate aero-dynamic forces on a soil surface, Trans., AGU, 39(3), 397-404.

Goto, T., Kitamura, T. and Tsujimoto, T. 2001. Study on bed-degradation and bank-erosion in straight gravel channel due to changes in boundary conditions. Journal of Hydraulic, Coastal and Environmental Engineering. JSCE, 684(II-56), 35-46 (in Japanese).

Hasegawa, K. 1984. Hydraulic research on planimetric forms, bed topographies and flow in alluvial rivers. PhD Dissertation, Hokkaido University (in Japanese).

Kovacs, A. and Parker, G. 1994. A new vectorial bedload formulation and its application to the time evolution of straight river channels. Journal of Fluid Mech., 267, 153-183.

Leonard, B.P. 1979. A stable and accurate convective modelling procedure based on quadratic upstream interpolation, Computer Methods in Applied Mechanics and Engineering, 19(1), 59-98.

Meguro, H., Hasegawa, K., Ohtsuka, T. and Tatsuzawa, H. 2001. Experimental reproduction of superposed large-, medium- and small-scale bed forms found in mountain rivers. Annual Journal of Hydraulic Engineering, 45, 733-738 (in Japanese).

Nagata, N., Hosoda, T., Muramoto, Y. and Rahman, Md. M. 1996. Numerical analysis of channel processes with bank erotion by means of moving boundary fitted coordinate system. Annual Journal of Hydraulic Engineering, 40, 927-932 (in Japanese).

Nagata, N., Hosoda, T. and Muramoto, Y. 2000. Numerical analysis of river channel processes with bank erosion. Journal of Hydraulic Engineering, ASCE, 126(4), 243-252.

Nakagawa, H. and Tsujimoto, T. 1980. Sand bed instability due to bed load motion, Journal of Hydraulics Division. ASCE, 106(HY12), 2029-2051.

Nakagawa, H., Tsujimoto, T. and Murakami, S. 1986. Non-equilibrium bed load transport along side slope of an alluvial stream. Proc. of 3rd Int. Symp. on River Sedimentation, 885-893.

Nils Reidar B. and Olsen, M. 2003. Three-dimensional CFD modeling of self-forming meandering channel. Journal of Hydraulic Engineering, ASCE, 129(5), 366-372.

Sekine, M. 1996. Study on the channel migration due to a bank erosion. Journal of Hydraulic, Coastal and Environmental Engineering. JSCE, 533(II-34), 51-59 (in Japanese).

Sekine, M. 2004. Numerical simulation of braided stream formation on the basis of slope-collapse model. Journal of Hydroscience and Hydraulic Engineering, JSCE, 22(2), 1-10.

Seminara, G. 2006. Meanders. Journal of Fluid Mech., 554, 271-297.

Shimizu, Y., Hirano, M. and Watanabe, Y. 1996. Numerical calculation of bank erosion and free meandering. Annual Journal of Hydraulic Engineering, 40, 921-926 (in Japanese).

Shimizu, Y. 2004. Mutual effects of bed and bank deformation in channel plane formation. Journal of Hydroscience and Hydraulic Engineering, JSCE, 22(2), 25-35.